Through Over-Clad Inscription of FBG in CYTOP Optical Fiber Using Phase Mask Technique and 400 nm Femtosecond Pulsed Laser

Ying-Gang Nan, *Student Member, IEEE*, Ivan Chapalo, Karima Chah, Xuehao Hu, and Patrice Mégret

***Abstract*—In this work, we report the inscription of fiber Bragg grating through the over-clad in cyclic transparent fluoropolymer (CYTOP) optical fiber using a phase mask technique and a 400 nm femtosecond pulsed laser. 8 mm-long grating were obtained in less than 20 s with 500 μW average beam power. To investigate the FBG properties and discriminate between the protective over-clad influence and the core-cladding effect, we inscribe FBGs in the fiber with and without the over-clad. We also show that the temperature sensitivity of CYTOP-FBGs with the over-clad depends on the relative humidity, whereas CYTOP-FBGs without the over-clad achieve almost zero sensitivity to humidity and sensitivity to temperature of 26.7 pm/°C.**

***Index Terms*—Fiber Bragg gratings (FBGs), phase mask technique, femtosecond laser, CYTOP, with over-clad.**

I. Introduction

DUE to the significant advantages such as low Young's modulus, biocompatibility and high flexibility, polymer optical fibers (POFs) attracts more and more attention in the fields of communication and sensing devices [1]–[8]. Among POFs, CYTOP fiber is a good candidate for such applications due to its low attenuation in telecom transparency windows and specific material properties [9]–[13]. For sensing purposes, fiber Bragg gratings (FBGs) is one of the most efficient and convenient technology [2], [14]. Therefore, FBG inscription in CYTOP fiber plays a critical role in achieving gratings with specific properties that meet the application requirements.

Two methods of FBGs inscription in CYTOP fiber are currently routinely used: the phase mask [4], [15], [16], and the direct inscription [17]–[19]. For the direct inscription method, a series of essential results of FBGs inscription with highly flexible parameters have been demonstrated using femtosecond (fs) laser operating at 517 nm [17], [18]. Recently, we demonstrated and characterized the fs inscription at 800 nm as well [19]. The significant advantages of the 517 nm or 800 nm direct fs technique are the possibility of through over-clad inscription keeping the fiber integrity, and the flexibility to realize a custom FBG design. This writing technique is possible because the over-clad is transparent in the visible and near infrared spectral ranges. At the same time, the direct inscription process requires a tight focusing of the laser beam through a high numerical aperture (NA) microscope objective and an accurate control of the beam position in the fiber core that requires expensive high precision automated translation stages. The alignment and inscription steps may take a long time especially when line by line or plane by plane methods are used [19].

FBGs inscription by phase masks is a well-known classic method that does not require such a high precise and expensive positioning equipment. Two kinds of lasers are reported for a phase mask FBGs inscription in CYTOP: 248 nm Krypton Fluoride (KrF) excimer laser [15], [16] and 400 nm fs pulsed laser [4]. Gratings fabricated by the excimer laser show a relatively low reflectivity, broad reflection peak (9 nm to 10 nm), and require long exposure time (up to 60 min) [15], [16]. For a successful inscription, the over-clad must be removed, and this process takes time and disturbs the fiber integrity and durability [4], [15], [16]. For 400 nm fs laser, we recently reported a reflectivity up to 92% obtained in a drastically reduced exposure time (10 s). Moreover, the full width at half maximum bandwidth was also reduced to less than 0.5 nm for 2 mm-long gratings, showing that reflection peaks corresponding to different mode groups do not overlap. Nevertheless, the over-clad of the fiber was also removed before the inscription due to the low damage threshold of the over-clad [4]. This pretreatment and sample preparation is again time consuming and makes CYTOP fiber more fragile. Thus, it is essential to enhance this method in order to provide through over-clad fast inscription of CYTOP-FBGs with high reflectivity, good repeatability, and preserving the fiber integrity.

For any CYTOP-FBG application, it is necessary to perform FBGs characterization, and, in particular, to determine their sensitivities to physical quantities such as temperature and relative humidity. To date, a series of works reporting on CYTOP-FBGs characterization are published [4], [15], [16], [19], [20]. These articles can be classified into two categories: papers dealing with fibers with an over-clad [19], [20] and those dealing with

Manuscript received October 27, 2021; revised December 20, 2021; accepted January 14, 2022. Date of publication January 19, 2022; date of current version May 2, 2022. This work was supported by the Fonds de la Recherche Scientifique-FNRS under Grant T.0163.19 "RADPOF". *(Corresponding author: Ying-Gang Nan.)*

Ying-Gang Nan, Ivan Chapalo, Karima Chah, and Patrice Mégret are with the Electromagnetism and Telecommunication Department, University of Mons, 7000 Mons, Belgium (e-mail: yinggang.nan@umons.ac.be; Ivan.CHAPALO@umons.ac.be; Karima.CHAH@umons.ac.be; patrice.megret@umons.ac.be).

Xuehao Hu is with the Research Center for Advanced Optics and Photoelectronics, Department of Physics, College of Science, Shantou University, Shantou, Guangdong 515063, China (e-mail: xhhu3@stu.edu.cn).

Color versions of one or more figures in this article are available at https://doi.org/10.1109/JLT.2022.3144029.

Digital Object Identifier 10.1109/JLT.2022.3144029

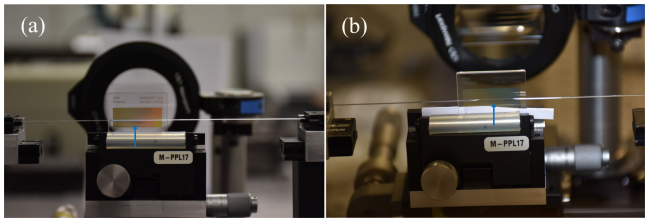

Fig. 1. The CYTOP fiber: (a) with over-clad; (b) without over-clad.

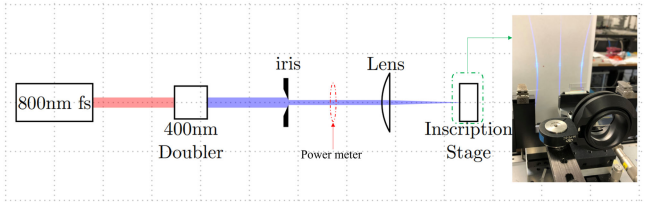

Fig. 2. Experimental setup to inscribe FBG in CYTOP with and without over-clad.

fibers without an over-clad [4], [15], [16]. However, there is no study comparing properties of CYTOP-FBG inscribed with and without an over-clad by the same inscription method and characterized under the same experimental conditions. For FBGs in CYTOP with over-clad, the reported sensitivities to temperature and humidity are 17.62 pm/°C and 14.7 pm/%RH in [20], and 37.3 pm/°C and 22.3 pm/%RH in [19], whereas without over-clad, the sensitivities to temperature and humidity are 27.5 $\pm$ 2.4 pm/°C and 10.3 $\pm$ 1.8 pm/%RH, respectively [4], [16].

In this work, we report for the first time to the best of our knowledge, FBG inscription through the over-clad in CYTOP fiber using a 400 nm fs pulsed laser and a phase mask. We show that the proposed technique has a high repeatability and an inscription time as low as 20 s. To investigate the over-clad effect on FBG properties, the same inscription setup was used to produce FBGs in CYTOP fibers where the polycarbonate-based over-clad was removed on a length of 2 cm by dichloromethane CH_2Cl_2 in 10 min [4], [21], [22]. We characterize both CYTOP-FBG types versus temperature in the range from 20 °C to 50 °C with steps of 5 °C (heating up) and -5 °C (cooling down), and versus humidity in the range 20 %RH to 60 %RH with steps of 20 %RH . We demonstrate that similar temperature sensitivities are found for CYTOP fibers with and without over-clad, whereas humidity sensitivities strongly depends on the presence or absence of the over-clad.

II. FBG Inscription

Fig. 1(a) and (b) represents the CYTOP fibers with and without over-clad. The FBG fabrication is performed with a femtosecond laser (a Mai Tai and Spitfire Pro. amplifier from Spectra Physics company) producing 120 fs light pulses at 800 nm with a repetition rate of 1 kHz and energy of 4 mJ. The laser is followed by a variable attenuator and a frequency doubler to deliver pulses at 400 nm. The laser beam diameter can be adjusted by an iris and focused onto the core of the CYTOP fiber through the phase mask by a plano-convex cylindrical lens with a focal length of 100 mm. The phase mask has a period of 1158 nm, and a powermeter is inserted between the lens and the diaphragm to measure the effective power of the inscription beam. A cover glass (from Corning) is put between the phase mask and the CYTOP fiber to protect the phase mask. Fig. 2 shows the experimental setup in this work.

An FBG interrogator (FS2200 from FiberSensing) with a spectral resolution of 1 pm and a spectral range from 1500 nm to 1600 nm is used to monitor FBG spectrum evolution in real-time. Moreover, a butt coupling between a standard single-mode silica optical fiber pigtail (SMF-28) and the CYTOP fiber is used as a link towards the interrogator. A small drop of refractive index matching gel ($n = 1.4646$ at 589.3 nm) is used between the two optical fibers to reduce Fresnel reflections from the interfaces of the SMF and CYTOP [4].

The commercially available graded-index CYTOP fiber (GigaPOF-62SR from Chromis) is used in this fabrication, with core diameter, over-clad diameter, and numerical aperture of 62.5 μm, 490 μm, and 0.185, respectively [23].

Although fabrication of high-quality FBGs in 50 μm core diameter CYTOP fiber without over-clad using phase mask technique is reported in [4], this inscription method is not suitable to fabricate FBG through the over-clad, unless we change the focusing lens to a higher numerical aperture one or to use larger core diameter fiber. Indeed, part of the high intensity inscription beam will be absorbed in the over-clad, that in turn leads to deformation of the periodic structure transferred to the core, as the polycarbonate-based over-clad has a lower fs-laser damage threshold than the CYTOP-based core material [4]. The focused average power for FBG inscription in the core may create huge damage in the over-clad of the CYTOP optical fiber. Moreover, we experimentally notice that the average beam intensity, and the exposure time are the main parameters that contribute to the damage effect of the over-clad. For example, for a 8 mm-long grating, the over-clad was damaged when exposure time was over 40 s with 500 μW average beam power. To avoid this damage, we can use high numerical aperture (NA) focusing lens so as to have a reduced Rayleigh length. Therefore, we can selectively focus the power in the fiber core as it is the case for the direct inscription methods [18], [19]. Another option is to use higher core diameter of the optical fiber. In this case, the Rayleigh length of the focusing lens where the density of power is the highest, is mostly covered by the core of the optical fiber. In this study, the CYTOP fiber used here has the same chemical composition and optical properties as in [4], but with a larger core diameter of 62.5 μm instead of 50 μm.

Fig. 3 shows a detailed view of the inscription system for the 62.5 μm core diameter CYTOP fibers.

In this work, the grating length is fixed at 8 mm, and the exposure time is decreased by increasing the average beam power. The beam is focused on the fiber core accurately by the plano-convex cylindrical lens to ensure the range of the double Rayleigh length is located at the core. Thus, more power of the beam will be focused on the fiber core rather than on the over-clad, minimizing the over-clad damage. Two optical parameters are used to analyze the fabrication of the FBGs in

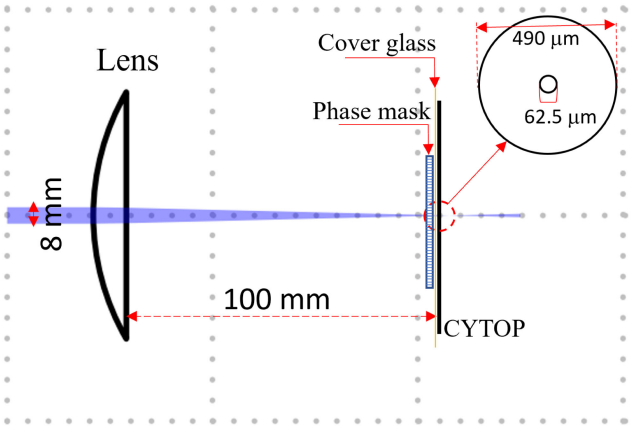

Fig. 3. The schematic of 8 mm beam diameter light system to inscribe FBG in 62.5 μm core diameter CYTOP fibers with over-clad.

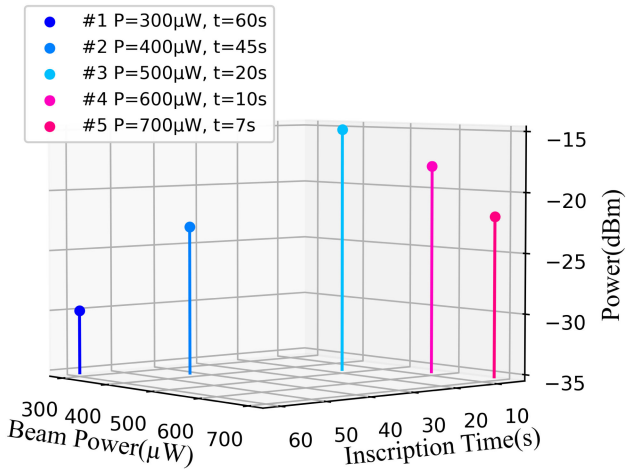

Fig. 4. The evolution of the fundamental peak power and the inscription time under different beam power for 8 mm-long grating in 62.5 μm core diameter CYTOP fibers with over-clad.

the CYTOP fibers. Firstly, the beam waist diameter (W) is used to determine the effective beam dimensions at the focus, and it is expressed by

$$W = \frac{2\lambda F}{\pi D} \tag{1}$$

where λ is the inscription wavelength, F is the focal length of the lens, and D is the beam diameter. The second parameter is the surface power density (I) to measure the amount of power per unit area that reaches the fiber core during the fabrication neglecting the material absorption. It is given by

$$I = \frac{P}{2DW} \tag{2}$$

where P is the beam average power.

Using the light system of Fig. 3, we fix the beam diameter to 8 mm and use different beam powers and exposure times to find the suitable inscription parameters for this CYTOP fiber. Fig. 4 shows the power reflected by the fundamental peak versus the inscription power and the exposure time. It is seen that the best reflection (grating #3) occurs for a beam power of 500 μW with an inscription time of 20 s. For FBG in 62.5 μm core diameter CYTOP fibers, this corresponds to a beam waist diameter of 3.18 μm, and a surface power density of 9.82×10^{-9} W/μm^2

TABLE I
THE DISTRIBUTION OF BRAGG RESONANCE WAVELENGTHS IN 62.5 μM CYTOP FIBER

m	n_m	λ_m (nm)
1	1.3405	1552.34
2	1.3395	1551.14
3	1.3384	1549.82
4	1.3373	1548.56
5	1.3362	1547.30
6	1.3351	1546.03
7	1.3340	1544.77
8	1.3330	1543.50
9	1.3218	1542.23
10	1.3207	1540.96
11	1.3296	1539.69

Due to the large core diameter, these CYTOP fibers are multimode [4], [15], [20] that leads to a well resolved multi-peak spectra whose peaks correspond to excited mode groups [4], [24], [25]. The mode group in parabolic-index fiber represents modes with approximately the same propagation constant. It is generally assumed that non ideal FBGs form spectra with additional intermediate reflection peaks located in the middle between adjacent main peaks [4], [25], [26]. They are referred to as cross-mode groups. In parabolic graded-index multimode fiber, the number of the mode groups is expressed as [4], [25]

$$M = \frac{V}{2}. \tag{3}$$

where $V = (2\pi a \mathrm{NA})/\lambda_0$ is the normalized frequency with $\mathrm{NA} = \sqrt{n_{\mathrm{co}}^2 - n_{\mathrm{cl}}^2} = n_{\mathrm{co}}\sqrt{2\Delta}$ the numerical aperture, and $\Delta = (n_{\mathrm{co}}^2 - n_{\mathrm{cl}}^2)/2n_{\mathrm{co}}^2$ is the index difference between the core and the cladding. Moreover, the effective refractive index n_m of the m^{th} mode group can be expressed as [4], [25], [27]

$$n_m = n_{\mathrm{co}}\sqrt{1 - 4m\Delta/\mathrm{V}}. \tag{4}$$

According to the Bragg wavelength equation $\lambda_{\mathrm{Bragg}} = 2n_{\mathrm{eff}}\Lambda$, the resonance wavelengths of the m^{th} mode group are given by

$$\lambda_m = 2n_m\Lambda \tag{5}$$

where Λ is the period of the grating. For 62.5 μm core diameter CYTOP fiber, $\mathrm{NA} \approx 0.185$, $n_{\mathrm{co}} \approx 1.342$, $a = 31.25$ μm, the period of grating is $\Lambda = 579$ nm, leading to $V \simeq 23.4$ and $M \simeq 11$ for λ_0 around 1550 nm. The values of the effective index and the resonance wavelength of each mode group are summarized in Table I.

Fig. 5(a) shows the #3 FBG spectra, where the black dotted lines represent the calculated resonance wavelength locations of the different mode groups described in Table I, and the first mode group (fundamental mode) is labelled by λ_1. It is clearly seen that the agreement between the experimental peaks of the spectrum and the computed resonance wavelengths is quite good. The experimental spectrum shows that the wavelength spacing between reflection peaks corresponding to adjacent mode groups is equal to 1.23 nm, and corresponds well to the theoretical value

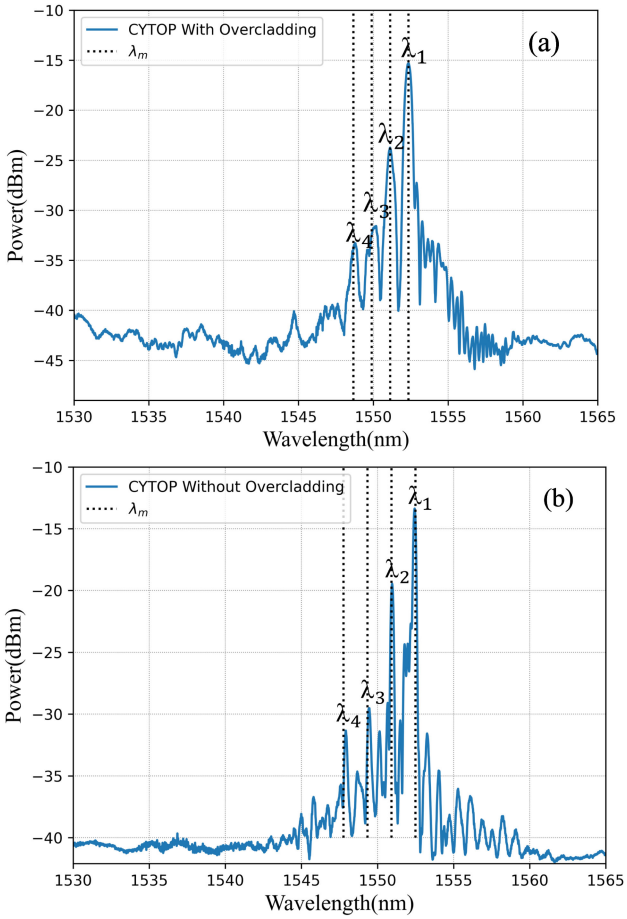

Fig. 5. Reflection spectra for two gratings: (a) grating #3 in 62.5 μm core diameter CYTOP with over-clad (inscription parameters: grating length 8 mm, laser power 500 μW, and inscription time 20 s); (b) grating #6 in 50 μm core diameter CYTOP without over-clad (inscription parameters: grating length 5 mm, laser power 100 μW, and inscription time 10 s).

computed by [4], [25]

$$\Delta\lambda = \frac{\lambda_0^2 \mathrm{NA}}{2\pi a n_{\mathrm{co}}^2}. \tag{6}$$

For comparison, Fig. 5(b) shows the reflection spectrum for the FBG (labelled #6) made in 50 μm core CYTOP fiber but with removed over-clad [4]. Here wavelength spacing between two adjacent mode groups $\Delta\lambda$ is 1.57 nm, which again corresponds to the theoretical value.

To investigate the CYTOP-FBG stability, we monitored the reflection spectra of grating #3 for approximately 42 days, as shown in Fig. 6. The reason for the difference of the background level is the variable surface quality of the connection between the CYTOP fiber and the SMF-28 pigtail in each measurement. The power of the fundamental peak (λ_1) has approximately a 0.5 dB decrease, and then is stable after 28 days. Due to the SMF-CYTOP structure used to measure the FBG spectra, the connection fiber face of SMF and CYTOP also influences the power of the fundamental peak, and more importantly the launching conditions from single-mode to multimode fibers change the power distribution in the spectra [4]. Measuring the spectral behavior of FBG in MMF is therefore highly dependent

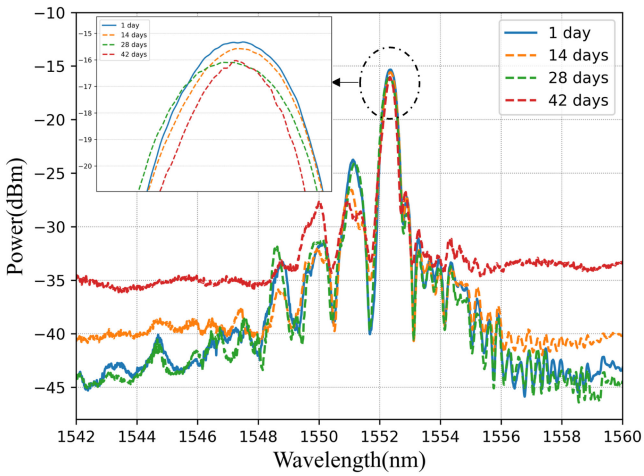

Fig. 6. FBG spectra evolution of grating #3 after fabrication.

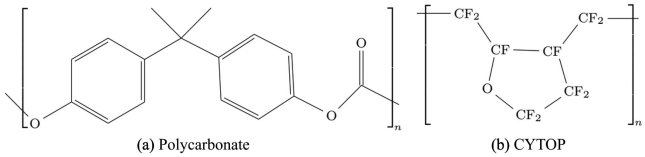

Fig. 7. Molecular structure: (a) polycarbonate-based over-clad; (b) pure CYTOP material.

on the launching conditions, and specially on the SMF-MMF connection. On the other hand, the launching conditions do not influence the chemical and mechanical stability of the inscribed FBGs. Consequently, for a given FBG, it could be difficult to get reproducible spectra when the launching conditions are variable from measurement to measurement. In our setup, we carefully fixed the launching conditions to always have the maximum reflected power in the fundamental mode peak (λ_1). Therefore, after reconnecting the CYTOP with SMF, the spectra will show approximately the same profile when the same launching conditions are chosen. Considering the connection error of the fiber face, Fig. 6 demonstrates that the grating inscribed in CYTOP fiber with over-clad using phase mask technique and 400 nm femtosecond laser is found very stable with time.

III. FBG Characteristics in CYTOP With and Without Over-Clad

Fig. 7(a) and (b) represents the chemical formula of the polycarbonate [28] based over-clad and the CYTOP fiber core materials [29].

From the data sheets of these polymer materials, the contact angles at 25 °C of water among polycarbonate and CYTOP are 82° [30] and 110° [31], respectively. Therefore, polycarbonate material shows hydrophilicity, whereas CYTOP material shows hydrophobicity. Then, although the perfluorinated polymer (CYTOP) is a hydrophobic material, the CYTOP fiber with its polycarbonate over-clad may show sensitivity to humidity as reported in [12], [19], [20]. On the other hand, a fiber without

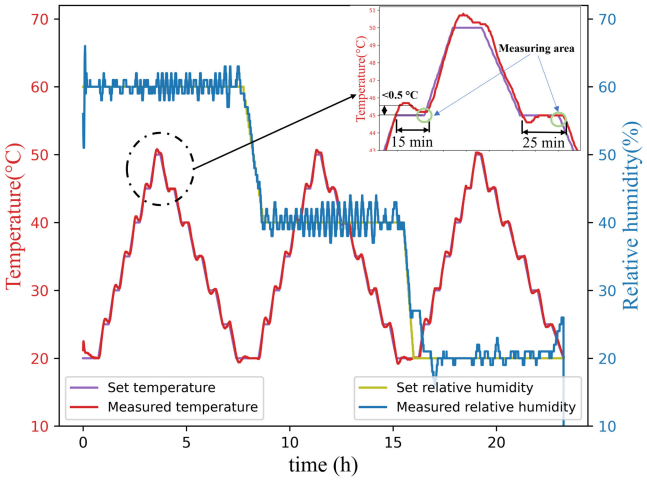

Fig. 8. Temperature and humidity cycles used to test the gratings in CYTOP with and without over-clad.

TABLE II
TEMPERATURE AND HUMIDITY SENSITIVITIES OF FBG IN CYTOP WITH AND WITHOUT OVER-CLAD

Environmental Conditions	Sensitivities	
Temperature or humidity	With over-clad	Without over-clad
60 %RH	32.2 pm/°C	26.8 pm/°C
40 %RH	29.2 pm/°C	26.7 pm/°C
20 %RH	27.2 pm/°C	26.8 pm/°C
45 °C	14.0 pm/%RH	<1 pm/%RH
35 °C	12.8 pm/%RH	<1 pm/%RH
25 °C	11.8 pm/%RH	<1 pm/%RH

over-clad should be nearly humidity insensitive, but nevertheless, a humidity sensitivity of 10.3 ± 1.8 pm/%RH was reported in [16] for a CYTOP-FBG without over-clad.

To investigate and compare the temperature and humidity sensitivities of CYTOP-FBGs with and without over-clad, we conducted experimental tests with a climate chamber (Weiss SB 22 [32]) to set and control the temperature and humidity during the experiment. Fig. 8 displays the three temperature cycles (from 20 °C to 50 °C) with steps of 5 °C (heating up) and −5 °C (cooling down), and the humidity (from 20 %RH to 60 %RH) with three fixed values of 60 %RH, 40 %RH, and 20 %RH that were used in this work. The time to make one complete cycle is approximately 24 h, and the experiment is repeated three times. As shown in the inset of Fig. 8, the FBG spectra are recorded 10 min after setting up each heating up step, and 20 min after each cooling down step, as more stabilization time is needed in the cooling down process [4], [19].

It was shown in [4] that the temperature sensitivities for the different mode groups and cross-mode groups are the same; therefore we only monitor the wavelength shift of the first mode group λ_1 to compute the FBG response to temperature and humidity of grating #3 (with over-clad) and #6 (without over-clad).

Fig. 9 shows the temperature response of the CYTOP-FBG with over-clad for three humidity levels from which the temperature sensitivities are computed (first three lines, second column of Table II).

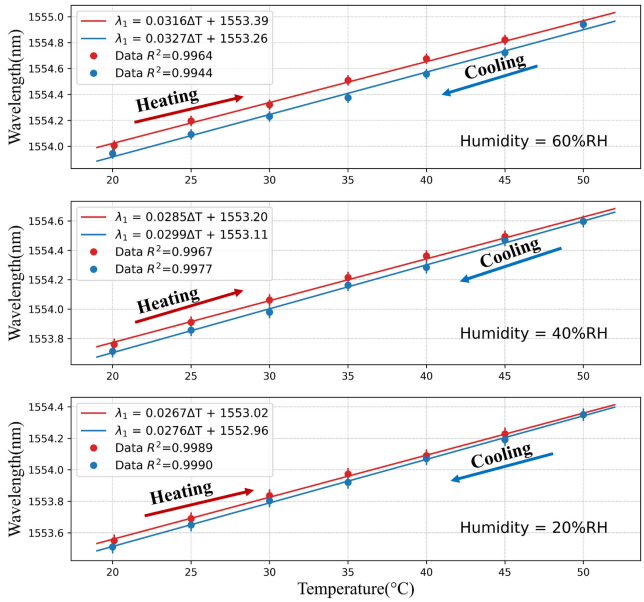

Fig. 9. Temperature response of the first mode group λ_1 of grating #3 for different humidity levels in CYTOP with over-clad.

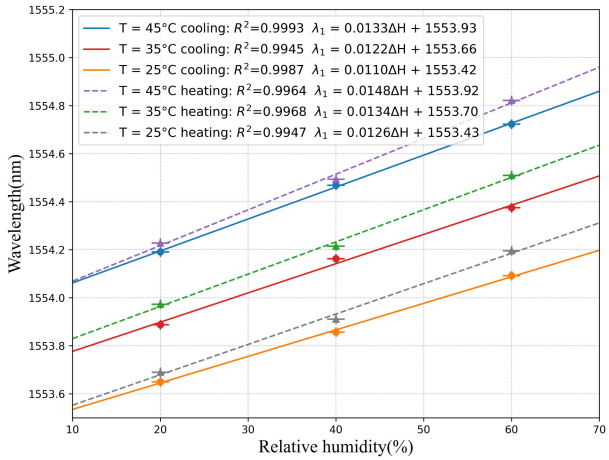

Fig. 10. Humidity response of the first mode group λ_1 of grating #3 for different temperature levels in CYTOP with over-clad.

It is clear that the first mode group evolves linearly with the change of temperature for different humidity levels with a coefficient of determination R^2 always better than 0.99. For a given humidity level, approximately the same temperature sensitivity is found in both heating and cooling processes. However, temperature sensitivities are humidity dependent, ranging from 32.2 pm/°C for 60 %RH to 27.2 pm/°C for 20 %RH . Decreasing the humdity level decreases the temperature sensitivity, for CYTOP fiber with over-clad.

Fig. 10 shows the humidity response of the CYTOP-FBG with over-clad for three temperature levels from which the humidity sensitivities are computed (last three lines, second column of Table II). Again, the linear fit is very good with a coefficient of determination R^2 always better than 0.99. It is noted that increasing the temperature, slightly increases the humidity sensitivity.

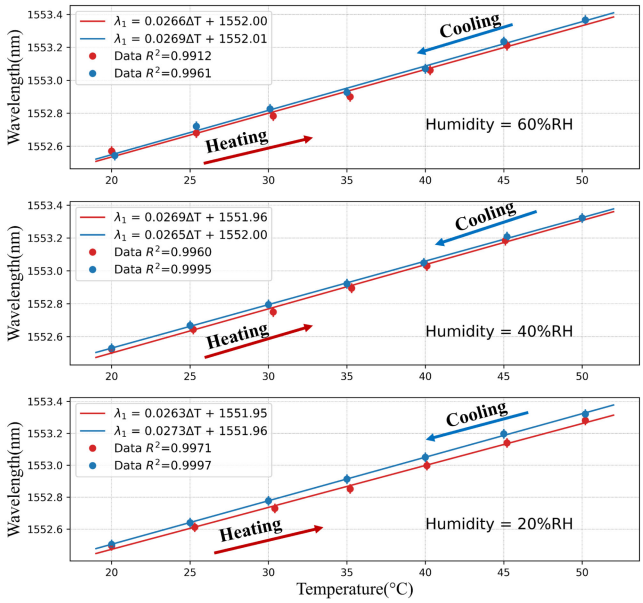

Fig. 11. Temperature response of first mode group λ_1 of grating #6 for different humidity levels in CYTOP without over-clad.

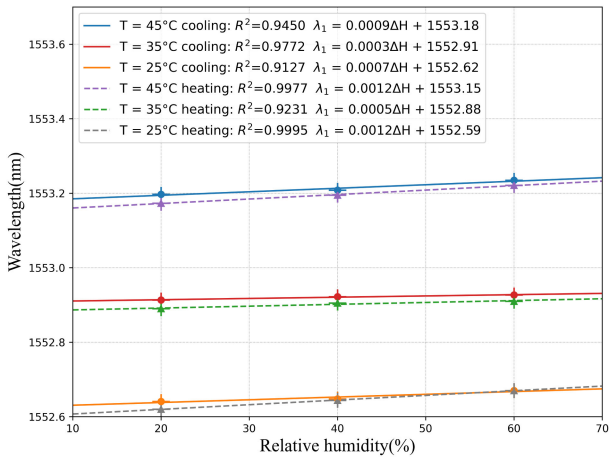

Fig. 12. Humidity response of the first mode group λ_1 of grating #6 for different humidity levels in CYTOP without over-clad.

The main outcome of this experiment is that the temperature and the humidity sensitivities are correlated with the CYTOP-FBG's polycarbonate over-clad, due to its hydrophilicity. This reason may probably explain the different temperature and humidity sensitivities found in different articles [4], [15], [16], [18], [19].

We repeated the same experiments with the CYTOP-FBG without the over-clad (grating #6). The results are presented in Fig. 11 for the temperature response at three humidity levels, and in Fig. 12 for the humidity response at three temperature levels. The computed sensitivities are summarized in Table II (first three lines, third column for the temperature sensitivities and last three lines, third column for the humidity sensitivities).

It is clearly seen that the first mode group evolves linearly with the change of temperature for different humidity levels with a coefficient of determination R^2 always better than 0.99. For a given humidity level, the same temperature sensitivity is found in both heating and cooling processes. Contrary to CYTOP-FBG with over-clad, temperature sensitivities are not humidity dependent, with a value around 26.7 pm/°C for all humidity levels. Moreover, contrary to [16], there is negligible humidity sensitivity (<1 pm/%RH) for all temperature levels. Compared with the grating in the CYTOP fiber without the over-clad, CYTOP-FBG with over-clad are humidity sensitive. This can be explained by the fact that the over-clad absorbs water molecules and swells, which in turn strains the fiber and induces Bragg wavelength shift. For different humidity levels, the induced strain is different, also leading to different temperature sensitivities.

IV. Conclusion

In summary, we have successfully written FBGs in CYTOP through the over-clad by using the phase mask technique and a femtosecond pulsed laser emitting at 400 nm. A 8 mm-long grating was achieved in only 20 s with an average beam power of 500 μW. This inscription method combines the advantages of the phase mask technique and femtosecond laser system, to provide gratings of high quality, good repeatability, and in a few seconds. Moreover, the over-clad should not be removed, preserving the fiber integrity.

By using a reproducible SMF-MMF connection, long-term (42 days) monitoring of the reflection spectrum of the CYTOP-FBG with over-clad reveals a very good stability, with less than 0.5 dB variation.

The comparison of the temperature and humidity sensitivities for CYTOP-FBG with and without polycarbonate over-clad highlights the importance of the hydrophilic properties of over-clad material. Indeed, without over-clad, gratings are nearly humidity insensitive leading to humidity independent temperature sensitivities, whereas gratings with over-clad are humidity sensitive that translates to temperature sensitivities that are also humidity dependent.

References

[1] J. N. Dash, X. Cheng, D. S. Gunawardena, and H.-Y. Tam, "Rectangular single-mode polymer optical fiber for femtosecond laser inscription of FBGs," *Photon. Res.*, vol. 9, no. 10, Oct. 2021, Art. no. 1931.

[2] C. Broadway, R. Min, A. G. Leal-Junior, C. Marques, and C. Caucheteur, "Toward commercial polymer fiber Bragg grating sensors: Review and applications," *J. Lightw. Technol.*, vol. 37, no. 11, pp. 2605–2615, Jun. 2019.

[3] J. Bonefacino *et al.*, "Ultra-fast polymer optical fibre Bragg grating inscription for medical devices," *Light: Sci. Appl.*, vol. 7, no. 3, pp. 17161–17171, Mar. 2017.

[4] Y.-G. Nan, D. Kinet, K. Chah, I. Chapalo, C. Caucheteur, and P. Mégret, "Ultra-fast fiber Bragg grating inscription in CYTOP polymer optical fibers using phase mask and 400 nm femtosecond laser," *Opt. Express*, vol. 29, no. 16, Aug. 2021, Art. no. 25824.

[5] M. Lobry *et al.*, "Multimodal plasmonic optical fiber grating aptasensor," *Opt. Express*, vol. 28, no. 5, Feb. 2020, Art. no. 7539.

[6] C. Broadway *et al.*, "CYTOP fibre Bragg grating sensors for harsh radiation environments," *Sensors*, vol. 19, no. 13, Jun. 2019, Art. no. 2853.

[7] A. Theodosiou, P. Savva, E. Mendoza, M. Petrou, and K. Kalli, "In-situ relative humidity sensing for ultra-high-performance concrete using polymer fiber Bragg gratings," *IEEE Sensors J.*, vol. 21, no. 14, pp. 16086–16092, Jul. 2021.

[8] X. Hu, D. Kinet, K. Chah, C.-F. J. Pun, H.-Y. Tam, and C. Caucheteur, "Bragg grating inscription in PMMA optical fibers using 400-nm femtosecond pulses," *Opt. Lett.*, vol. 42, no. 14, Jul. 2017, Art. no. 2794.

[9] A. Theodosiou and K. Kalli, "Recent trends and advances of fibre Bragg grating sensors in CYTOP polymer optical fibres," *Opt. Fiber Technol.*, vol. 54, Jan. 2020, Art. no. 102079.

[10] I. Chapalo, A. Theodosiou, K. Kalli, and O. Kotov, "Multimode fiber interferometer based on graded-index polymer CYTOP fiber," *J. Lightw. Technol.*, vol. 38, no. 6, pp. 1439–1445, Mar. 2020.

[11] A. Theodosiou *et al.*, "Long period grating in a multimode cyclic transparent optical polymer fiber inscribed using a femtosecond laser," *Opt. Lett.*, vol. 44, no. 21, Oct. 2019, Art. no. 5346.

[12] *Information on the detail of CYTOP material*. [Online]. Available: https://www.bellexinternational.com/products/cytop/

[13] A. Leal-Junior *et al.*, "Polymer optical fiber Bragg gratings in CYTOP fibers for angle measurement with dynamic compensation," *Polymers*, vol. 10, no. 6, Jun. 2018, Art. no. 674.

[14] Y. Mizuno, A. Theodosiou, K. Kalli, S. Liehr, H. Lee, and K. Nakamura, "Distributed polymer optical fiber sensors: A review and outlook," *Photon. Res.*, vol. 9, no. 9, pp. 1719–1733, Aug. 2021.

[15] M. Koerdt *et al.*, "Fabrication and characterization of Bragg gratings in perfluorinated polymer optical fibers and their embedding in composites," *Mechatronics*, vol. 34, pp. 137–146, 2016.

[16] Y. Zheng, K. Bremer, and B. Roth, "Investigating the strain, temperature and humidity sensitivity of a multimode graded-index perfluorinated polymer optical fiber with Bragg grating," *Sensors*, vol. 18, no. 5, 2018, Art. no. 1436.

[17] A. Lacraz, M. Polis, A. Theodosiou, C. Koutsides, and K. Kalli, "Femtosecond laser inscribed Bragg gratings in low loss CYTOP polymer optical fiber," *IEEE Photon. Technol. Lett.*, vol. 27, no. 7, pp. 693–696, Apr. 2015.

[18] A. Theodosiou, A. Lacraz, A. Stassis, C. Koutsides, M. Komodromos, and K. Kalli, "Plane-by-plane femtosecond laser inscription method for single-peak Bragg gratings in multimode CYTOP polymer optical fiber," *J. Lightw. Technol.*, vol. 35, no. 24, pp. 5404–5410, 2017.

[19] K. Chah, I. Chapalo, Y.-G. Nan, D. Kinet, P. Mégret, and C. Caucheteur, "800 nm femtosecond pulses for direct inscription of FBGs in CYTOP polymer optical fiber," *Opt. Lett.*, vol. 46, no. 17, pp. 4272–4275, Jul. 2021.

[20] A. Theodosiou, M. Komodromos, and K. Kalli, "Carbon cantilever beam health inspection using a polymer fiber Bragg grating array," *J. Lightw. Technol.*, vol. 36, no. 4, pp. 986–992, Feb. 2018.

[21] R. Min, B. Ortega, and C. Marques, "Fabrication of tunable chirped mPOF Bragg gratings using a uniform phase mask," *Opt. Express*, vol. 26, no. 4, pp. 4411–4420, Feb. 2018.

[22] J. Villatoro, D. Monzón-Hernández, and D. Luna-Moreno, "In-line optical fiber sensors based on cladded multimode tapered fibers," *Appl. Opt.*, vol. 43, no. 32, pp. 5933–5938, Nov. 2004.

[23] *Information on the detail of CYTOP GigaPOF62S*. [Online]. Available: https://fiberfin.com/custom/upload/File-1403278487.pdf

[24] T. Mizunami, T. Djambova, T. Niiho, and S. Gupta, "Bragg gratings in multimode and few-mode optical fibers," *J. Lightw. Technol.*, vol. 18, no. 2, pp. 230–235, Feb. 2000.

[25] Y. Liu, J. Lit, X. Gu, and L. Wei, "Fiber comb filters based on UV-writing Bragg gratings in graded-index multimode fibers," *Opt. Express*, vol. 13, no. 21, pp. 8508–8513, 2005.

[26] C. Lu and Y. Cui, "Fiber Bragg grating spectra in multimode optical fibers," *J. Lightw. Technol.*, vol. 24, no. 1, pp. 598–604, Jan. 2006.

[27] A. Ghatak and K. Thyagarajan, "Propagation characteristics of graded index fibers," in *Introduction to Fiber Optics*. Cambridge, England: Cambridge Univ. Press, 1998, pp. 173–195.

[28] K. Takeuchi, "Polycarbonates," in *Polymer Science: A Comprehensive Reference*. Amsterdam, Netherland: Elsevier, 2012, vol. 5 - Polycondensation, *ch. 5.16*, pp. 363–376.

[29] K. Takeya, Y. Ikegami, K. Matsumura, K. Kawase, and H. Uchida, "Optical evaluation of CYTOP, an amorphous fluoropolymer, in the terahertz frequency across a wide temperature range," *Appl. Phys. Express*, vol. 12, no. 4, Mar. 2019, Art. no. 042004.

[30] *The contact angle of polycarbonate polymer*. [Online]. Available: https://www.accudynetest.com/polytable_03.html?sortby=contact_angle

[31] *The contact angle of CYTOP polymer*. [Online]. Available: https://www.agcce.com/cytop-technical-information/

[32] *The information of Weiss SB 22 climate chamber*. [Online]. Available: https://www.geminibv.com/labware/weiss-sb22-160140-climate-chamber/